

# Light nuclei production in relativistic heavy ion collisions from the AMPT model

Kai-Jia Sun\* and Che Ming Ko†

*Cyclotron Institute and Department of Physics and Astronomy,  
Texas A&M University, College Station, Texas 77843, USA*

(Dated: July 3, 2020)

Based on an improved multiphase transport (AMPT) model, which gives a good description of proton production with a smooth quark matter to hadronic matter transition in relativistic heavy ion collisions, we study deuteron and triton production from the coalescence of nucleons at the kinetic freezeout of these collisions. For Au+Au collisions at center-of-mass energies  $\sqrt{s_{NN}}$  from 7.7 GeV to 200 GeV available at the Relativistic Heavy Ion Collider (RHIC), we find that the yield ratio  $N_t N_p / N_d^2$  of proton, deuteron, and triton is essentially a constant as a function of collision energy. Our result confirms the expectation that without a first-order quark to hadronic matter phase transition in the produced matter or its approach to the critical point of the QCD matter, this yield ratio does not show any non-monotonic behavior in its collision energy dependence.

PACS numbers: 12.38.Mh, 5.75.Ld, 25.75.-q, 24.10.Lx

## I. INTRODUCTION

Light nuclei, such as deuteron ( $d$ ), helium-3 ( ${}^3\text{He}$ ), triton ( ${}^3\text{H}$  or  $t$ ), helium-4 ( ${}^4\text{He}$ ), hypertriton ( ${}^3_\Lambda\text{H}$ ) and their antiparticles, have been observed in high energy nucleus-nucleus (AA), proton-nucleus (pA), and pp collisions at RHIC and the LHC [1–6]. Because of their potential role in the search for the critical point [7–9] of strongly interaction matter in heavy ion collisions [10–13], studying these loosely bound nuclei with binding energies much smaller than the temperature of the hot dense matter created in these collisions has recently received an increased attention [14–30]. Also, these studies are useful for understanding the production of light (anti)nuclei in cosmic rays and in dark matter experiments [31–34]. As to the use of light nuclei production to probe the QCD phase diagram in relativistic heavy ion collisions, it is mainly due to their composite structures that make their production mostly from nucleons close in phase space and thus sensitive to their correlations and density fluctuations [10–13]. In particular, it has been suggested in Refs. [10, 11] that the yield ratio  $N_t N_p / N_d^2$  of proton, deuteron, and triton in relativistic heavy ion collisions could show a non-monotonic dependence on the collision energy as a result of the enhanced density fluctuations due to the spinodal instability during a first-order quark to hadronic matter phase transition and/or the long-range correlation if the produced matter is close to the critical point of the QCD matter.

The production of light nuclei in relativistic heavy ion collisions has been studied in various models, including the statistical hadronization model [35, 36], the nucleon coalescence model [37, 38], and dynamical models based on the kinetic theory [39]. In the statistical hadronization model, the yields of light nuclei are determined at

the same chemical freeze-out temperature and baryon chemical potential as those for identified hadrons like protons, pions, kaons, etc., while their spectra are calculated from a blast-wave model at the hadronic kinetic freeze out when hadrons undergo their last collisions. This model has successfully described light nuclei production in Pb+Pb collisions at  $\sqrt{s_{NN}} = 2.76$  TeV at LHC [16]. In the coalescence model, light nuclei are formed at kinetic freeze out from nucleons that are close in phase space. There have been various ways of implementing the coalescence model in the literature, and these include the naive coalescence model based on the introduction of a phenomenological coalescence radius in phase space [37, 38], the phase-space coalescence model that takes into account the internal wave functions of light nuclei [40–43], and the coalescence model that further uses the phase-space information of nucleons from microscopic transport models [19, 44–47]. In dynamic models for light nuclei production, these nuclei are treated as explicit degrees of freedom, and their production and destruction during the hadronic evolution stage in heavy ion collisions are described by appropriate hadronic reactions with cross sections that satisfy the detailed balance relations [48–50]. In particular, the studies in Refs. [49, 50] have shown that the deuteron yield remains almost unchanged from the chemical freeze out to the kinetic freeze out as a result of the large deuteron production and destruction cross sections that keep the deuteron abundance in thermal and chemical equilibrium in the expanding hadronic matter with decreasing temperature but increasing baryon chemical potential. All above models have been used in understanding the recent data from the STAR Collaboration on deuteron and triton in Au+Au collisions at  $\sqrt{s_{NN}} = 7.7\text{--}200$  GeV [51–53]. For the thermal model, it gives a good description of the deuteron yield but overestimates the triton yield. None of these models can, however, reproduce the non-monotonic behavior or peak structure in the collision energy dependence of the yield ratio  $N_p N_t / N_d^2$ .

In the present work, we investigate the production of

\*kjsun@tamu.edu

†ko@comp.tamu.edu

deuteron and triton in most central ( $b < 3$  fm) Au+Au collisions at  $\sqrt{s_{\text{NN}}} = 7.7\text{-}200$  GeV by using the phase-space coalescence model based on kinetically freeze-out nucleons from an improved multiphase transport (AMPT) model [54, 55]. The AMPT model, which has been extensively used for studying various observables in heavy ion collisions at relativistic energies, includes the initial conditions from the HIJING model [56, 57], the parton cascade via the ZPC model [58], and the hadronic transport based on the ART model [59] as well as a spatial quark coalescence model that converts kinetically freeze-out quarks and antiquarks to the initial hadrons. Since the transition from the quark phase to the hadronic phase in AMPT is not a first-order or second-order one, the collision energy dependence of the yield ratio  $N_t N_p / N_d^2$  from this model serves as a baseline against which experimental data can be compared to see if additional physics inputs, such as a non-smooth phase transition in the produced matter is needed in the AMPT model.

This paper is organized as follows. In Sec. II, we give a brief description of the nucleon phase-space coalescence model. We then present in Sec. III the energy dependence of the yield ratios  $N_d/N_p$ ,  $N_t/N_p$ , and  $N_t N_p / N_d^2$  obtained from the coalescence model based on nucleons from the AMPT model. Finally, a conclusion is given in Sec. V.

## II. NUCLEON COALESCENCE MODEL IN PHASE SPACE

For deuteron production from an emission source of protons and neutrons, its number in the coalescence model is calculated from the overlap of the proton and neutron phase-space distribution functions  $f_{p,n}(\mathbf{x}, \mathbf{p})$  with the Wigner function  $W_d(\mathbf{x}, \mathbf{p})$  of the deuteron internal wave function [63], i.e.,

$$N_d = g_d \int d^3 \mathbf{x}_1 d^3 \mathbf{p}_1 d^3 \mathbf{x}_2 d^3 \mathbf{p}_2 f_n(\mathbf{x}_1, \mathbf{p}_1) \times f_p(\mathbf{x}_2, \mathbf{p}_2) W_d(\mathbf{x}, \mathbf{p}), \quad (1)$$

with  $g_d = 3/4$  being the statistical factor for forming a deuteron of spin 1 from two spin 1/2 proton and neutron. Using the Gaussian or harmonic oscillator wave function for the internal wave function of a deuteron, as usually assumed in the coalescence model for deuteron production, its Wigner function is

$$W_d(\mathbf{x}, \mathbf{p}) = 8 \exp\left(-\frac{x^2}{\sigma^2} - \sigma^2 p^2\right) \quad (2)$$

and is normalized according to  $\int d^3 \mathbf{x} \int d^3 \mathbf{p} W_d(\mathbf{x}, \mathbf{p}) = (2\pi)^3$ . In the above,  $\mathbf{x}$  and  $\mathbf{p}$  are, respectively, the relative coordinate and momentum of the two nucleons in a deuteron, defined together with their center-of-mass co-

ordinate  $\mathbf{X}$  and momentum  $\mathbf{P}$  by [43, 64, 65]

$$\begin{aligned} \mathbf{X} &= \frac{\mathbf{x}_1 + \mathbf{x}_2}{2}, & \mathbf{x} &= \frac{\mathbf{x}_1 - \mathbf{x}_2}{\sqrt{2}}, \\ \mathbf{P} &= \mathbf{p}_1 + \mathbf{p}_2, & \mathbf{p} &= \frac{\mathbf{p}_1 - \mathbf{p}_2}{\sqrt{2}}. \end{aligned} \quad (3)$$

The parameter  $\sigma$  in Eq. (2) is related to the root-mean-square radius  $r_d$  of deuteron by  $\sigma = \sqrt{4/3} r_d \approx 2.26$  fm and is much smaller than the size of the hadronic system considered in the present study. We note that using the more realistic Hulthén wave function [66] for the deuteron, which can be represented by 15 Gaussian functions with different size parameters [64], gives essentially the same deuteron yield because of its insensitivity to the deuteron size in relativistic heavy-ion collisions [10, 11].

Similarly, the number of tritons from the coalescence of two neutrons and one proton is given by

$$N_t = g_t \int d^3 \mathbf{x}_1 d^3 \mathbf{p}_1 d^3 \mathbf{x}_2 d^3 \mathbf{p}_2 d^3 \mathbf{x}_3 d^3 \mathbf{p}_3 f_n(\mathbf{x}_1, \mathbf{p}_1) \times f_n(\mathbf{x}_2, \mathbf{p}_2) f_p(\mathbf{x}_3, \mathbf{p}_3) W_t(\mathbf{x}, \boldsymbol{\lambda}, \mathbf{p}, \mathbf{p}_\lambda), \quad (4)$$

where  $g_t = 1/4$  is the statistical factor for the formation of a spin 1/2 triton from two spin 1/2 neutrons and one spin 1/2 proton. The triton Wigner function in the above equation is

$$W_t(\mathbf{x}, \boldsymbol{\lambda}, \mathbf{p}, \mathbf{p}_\lambda) = 8^2 \exp\left(-\frac{x^2}{\sigma_t^2} - \frac{\lambda^2}{\sigma_t^2} - \sigma_t^2 p^2 - \sigma_t^2 p_\lambda^2\right), \quad (5)$$

where  $\mathbf{x}$  and  $\mathbf{p}$  are defined as in Eq.(3), and  $\boldsymbol{\lambda}$  and  $\mathbf{p}_\lambda$  are the additional relative coordinate and momentum. The latter are defined together with the center-of-mass coordinate  $\mathbf{X}$  and momentum  $\mathbf{P}$  of the nucleons in triton by [43, 64, 65]

$$\begin{aligned} \mathbf{X} &= \frac{\mathbf{x}_1 + \mathbf{x}_2 + \mathbf{x}_3}{3}, & \boldsymbol{\lambda} &= \frac{\mathbf{x}_1 + \mathbf{x}_2 - 2\mathbf{x}_3}{\sqrt{6}}, \\ \mathbf{P} &= \mathbf{p}_1 + \mathbf{p}_2 + \mathbf{p}_3, & \mathbf{p}_\lambda &= \frac{\mathbf{p}_1 + \mathbf{p}_2 - 2\mathbf{p}_3}{\sqrt{6}}. \end{aligned} \quad (6)$$

The parameter  $\sigma_t$  in Eq.(5) is related to the root-mean-square radius  $r_t$  of triton by  $\sigma_t = r_t = 1.59$  fm [67]. We note that the coordinate transformations in Eq. (3) and Eq. (6) conserve the volume in phase space, instead of the volumes in coordinate and momentum spaces separately.

## III. LIGHT NUCLEI PRODUCTION FROM THE AMPT MODEL

In the present work, we use the improved AMPT model of Ref. [55], which gives a better description of baryon production in relativistic heavy ion collisions than the usual AMPT model, to provide the phase-space information of nucleons needed for the production of deuteron

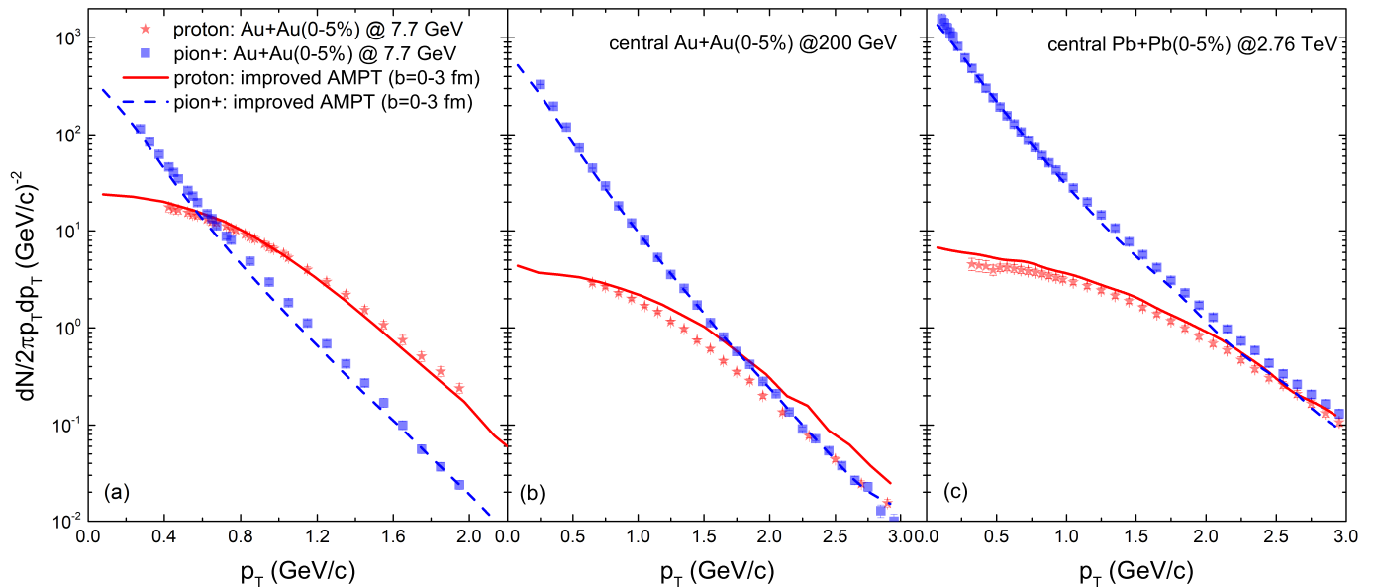


FIG. 1: (Color Online) Transverse momentum ( $p_T$ ) spectra of protons and pions in 0-5% central Au+Au and Pb+Pb collisions at  $\sqrt{s_{NN}} = 7.7$  GeV (panel (a)), 200 GeV (panel (b)), 2.76 TeV (panel (c)). Theoretical results are shown by solid lines for protons and dashed lines for pions, while the experimental data from Refs. [60–62] for protons and pions are denoted by solid stars and squares, respectively. Data for for protons at  $\sqrt{s_{NN}} = 200$  GeV and 2.76 TeV are corrected for the weak-decay contribution of hyperons.

and triton via the coalescence model. Specifically, from the kinetically freeze-out nucleons given by the AMPT with each one having a freeze-out position, momentum and time, the probability for a proton and a neutron to form a deuteron is calculated from Eq.(1) by using their relative coordinate and momentum obtained after free streaming the nucleon with an earlier freeze-out time to the later freeze-out time of the other nucleon. The similar procedure is used in calculating the probability from Eq.(4) for two neutrons and one proton to coalesce into a triton, i.e., by free streaming the two nucleons of earlier freeze-out times to the last freeze-out time of the remaining nucleon.

We first show in Fig. 1 the transverse momentum ( $p_T$ ) spectra of protons (solid lines) and pions (dashed lines) in 0-5% central Au+Au and Pb+Pb collisions at  $\sqrt{s_{NN}} = 7.7$  GeV (panel (a)), 200 GeV (panel (b)), and 2.76 TeV (panel (c)) obtained from the theoretical calculations. They are seen to describe fairly well the experimental data from Refs. [60–62], shown by solid stars and squares for protons and pions, respectively, confirming the success of the improved AMPT model of Ref. [55] in describing proton production in relativistic heavy ion collisions at both RHIC and the LHC.

We then show in the left window of Fig. 2 the yield ratio  $N_d/N_p$  ( $d/p$ ) of deuteron to proton and  $N_t/N_p$  ( $t/p$ ) of triton to proton as functions of the collision energy  $\sqrt{s_{NN}}$ . Results from the AMPT model, denoted by lines with solid squares, are seen to overestimate the measured  $d/p$  ratio (solid stars) by about a factor of 3 and  $t/p$  ratio (open stars) by about a factor of 9 for all colli-

sion energies from 7.7 GeV to 200 GeV. The overestimation of deuteron production has also been noticed in Ref. [44] based on an earlier version of the AMPT model. This failure is related to the low local temperature of initial hadrons at the hadronization in AMPT, which then leads to a similarly too low a temperature for nucleons at the kinetic freeze out. We note that for a given number of nucleons, a lower temperature results in a larger nucleon density in momentum space and thus enhances the production of deuteron and triton. Since the low local temperature is accompanied by a large radial flow in AMPT, the resulting proton transverse momentum spectrum can still reproduce the experimental data as shown in Fig. 1. To describe simultaneously the transverse momentum spectra of proton, deuteron and triton requires further improvements on the treatment of hadronization in AMPT, which is, however, beyond the scope of present study.

Right window of Fig. 2 shows the yield ratio  $N_p N_t / N_d^2$  as a function of the collision energy  $\sqrt{s_{NN}}$ . It is seen that this ratio has almost a constant value of around 0.4, which is slightly larger than the value of around 0.29 obtained by assuming a uniform distribution of nucleons in the analytical calculations of Refs. [10, 11]. Since this yield ratio is insensitive to the temperature and volume of the kinetic freeze-out hypersurface, the overestimation of the  $d/p$  and  $t/p$  ratios is not expected to have a large effect on this ratio. Indeed, the overestimation factors of 3 and 9 obtained in the above for the calculated  $d/p$  and  $t/p$  ratios cancel exactly in the  $N_p N_t / N_d^2$  ratio. The almost collision energy independent yield ratio

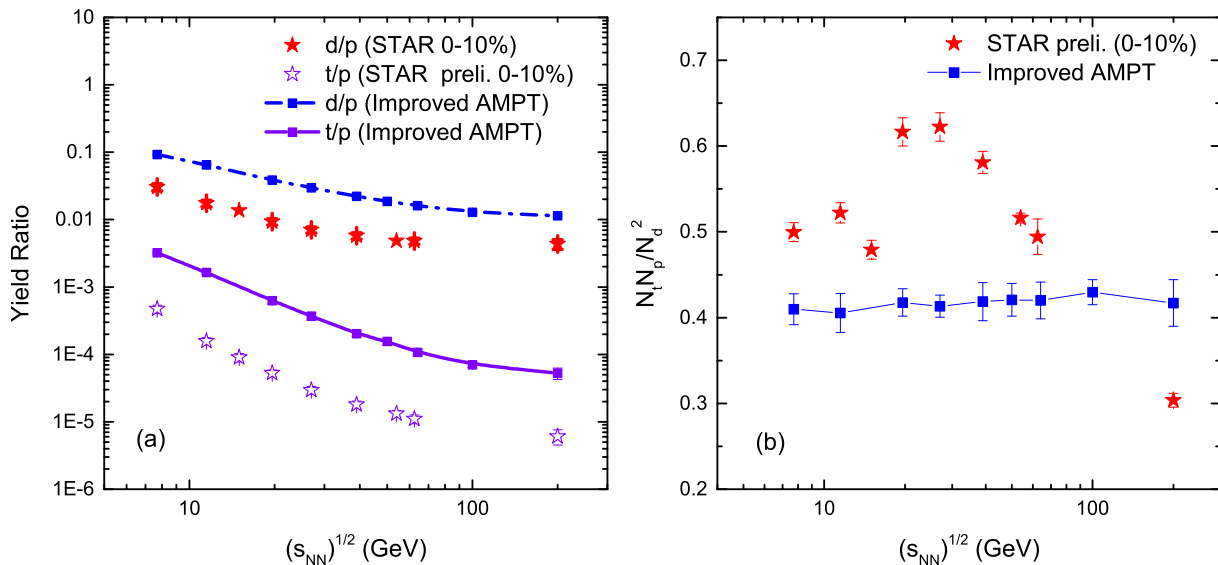


FIG. 2: (Color Online) The yield ratio  $N_d/N_p$  of deuteron to proton and  $N_t/N_p$  of triton to proton (left window) as well as the yield ratio  $N_t N_p / N_d^2$  (right window) as functions of the collision energy  $\sqrt{s_{NN}}$  in central Au+Au collisions. Results from the AMPT model are denoted by lines with solid squares, and experimental data from Refs. [45, 51–53] are shown by solid and open stars after correcting the weak-decay contribution from hyperons to protons [68].

$N_t N_p / N_d^2$  obtained in the present study contradicts the non-monotonic behavior seen in the data, shown by solid stars in the right window of Fig. 2. This result supports the suggestion in Refs. [10–13] that a non-monotonic dependence of this ratio on the energy of heavy ion collisions requires a first-order phase transition in the produced matter or the approach to the critical point of the QCD matter. Our result is similar to that in a recent study [45] using a pure hadronic JAM transport model with a coalescence model based simply on some coalescence radii in phase space, where the predicted value of the yield ratio  $N_t N_p / N_d^2$  is also almost a constant as a function of collision energy. The behavior of the yield ratio  $N_p N_t / N_d^2$  is thus insensitive to the details of the coalescence model. Our results can therefore be used as a baseline for understanding the background contribution in the search for the QCD critical point from heavy ion collisions in the beam energy scan (BES) program at RHIC.

#### IV. CONCLUSIONS

In the present work, we have studied light nuclei production from Au+Au collision at  $\sqrt{s_{NN}} = 7.7 - 200$  GeV

in the nucleon coalescence model based on the phase-space distribution of nucleons from the kinetically freeze out of an improved AMPT model. We have found that the yield ratio  $N_t N_p / N_d^2$  is essentially a constant as a function of collision energy. Since the AMPT model only has a smooth crossover from partonic matter to hadronic matter, our results provide the baseline for understanding the background contribution to the yield ratio  $N_t N_p / N_d^2$  in the BES program at RHIC. A deviation of experimentally measured collision energy dependence of this ratio from our results could hint at the occurrence of a non-smooth phase transition in the produced matter from these collisions and thus help to determine the location of the critical point in the QCD phase diagram.

#### Acknowledgments

The authors thank Ziwei Lin, Xiaofeng Luo, Hui Liu, and Shanshan Cao for helpful discussions. This work was supported in part by the U.S. Department of Energy under Contract No. de-sc0015266 and the Welch Foundation under Grant No. A-1358.

- 
- [1] B. I. Abelev et al. (STAR), *Science* **328**, 58 (2010), 1003.2030.  
 [2] H. Agakishiev et al. (STAR), *Nature* **473**, 353 (2011), [Erratum: *Nature*475,412(2011)], 1103.3312.

- [3] N. Sharma (ALICE), *J. Phys.* **G38**, 124189 (2011), 1109.4836.  
 [4] J. Adam et al. (STAR), *Nature Phys.* **16**, 409 (2020), 1904.10520.

- [5] S. Acharya et al. (ALICE) (2019), 1910.14401.
- [6] S. Acharya et al. (ALICE) (2020), 2003.03184.
- [7] A. Bzdak, S. Esumi, V. Koch, J. Liao, M. Stephanov, and N. Xu (2019), 1906.00936.
- [8] X. Luo, S. Shi, N. Xu, and Y. Zhang, *Particles* **3**, 278 (2020), 2004.00789.
- [9] D. Oliinychenko, in *28th International Conference on Ultrarelativistic Nucleus-Nucleus Collisions (Quark Matter 2019) Wuhan, China, November 4-9, 2019* (2020), 2003.05476.
- [10] K.-J. Sun, L.-W. Chen, C. M. Ko, and Z. Xu, *Phys. Lett.* **B774**, 103 (2017), 1702.07620.
- [11] K.-J. Sun, L.-W. Chen, C. M. Ko, J. Pu, and Z. Xu, *Phys. Lett.* **B781**, 499 (2018), 1801.09382.
- [12] E. Shuryak and J. M. Torres-Rincon, *Phys. Rev.* **C100**, 024903 (2019), 1805.04444.
- [13] E. Shuryak and J. M. Torres-Rincon (2019), 1910.08119.
- [14] Y.-G. Ma, J.-H. Chen, and L. Xue, *Front. Phys.(Beijing)* **7**, 637 (2012), 1301.4902.
- [15] A. Andronic, P. Braun-Munzinger, K. Redlich, and J. Stachel, *Nature* **561**, 321 (2018), 1710.09425.
- [16] P. Braun-Munzinger and B. Dönigus, *Nucl. Phys.* **A987**, 144 (2019), 1809.04681.
- [17] J. Chen, D. Keane, Y.-G. Ma, A. Tang, and Z. Xu, *Phys. Rept.* **760**, 1 (2018), 1808.09619.
- [18] S. Bazak and S. Mrowczynski, *Mod. Phys. Lett.* **A33**, 1850142 (2018), 1802.08212.
- [19] Z.-J. Dong, G. Chen, Q.-Y. Wang, Z.-L. She, Y.-L. Yan, F.-X. Liu, D.-M. Zhou, and B.-H. Sa, *Eur. Phys. J.* **A54**, 144 (2018), 1803.01547.
- [20] F. Bellini and A. P. Kalweit, *Phys. Rev.* **C99**, 054905 (2019), 1807.05894.
- [21] K.-J. Sun, C. M. Ko, and B. Dönigus, *Phys. Lett.* **B792**, 132 (2019), 1812.05175.
- [22] Y. Cai, T. D. Cohen, B. A. Gelman, and Y. Yamauchi, *Phys. Rev.* **C100**, 024911 (2019), 1905.02753.
- [23] S. Mrowczynski and P. Slon (2019), 1904.08320.
- [24] M. Kachelriess, S. Ostapchenko, and J. Tjemsland, *Eur. Phys. J.* **A56**, 4 (2020), 1905.01192.
- [25] S. Mrowczynski (2020), 2004.07029.
- [26] B. Dönigus, *Int. J. Mod. Phys.* **E29**, 2040001 (2020), 2004.10544.
- [27] T. Shao, J. Chen, C. M. Ko, K.-J. Sun, and Z. Xu (2020), 2004.02385.
- [28] V. Vovchenko, B. Dönigus, B. Kardan, M. Lorenz, and H. Stoecker (2020), 2004.04411.
- [29] Y. Ye, Y. Wang, Q. Li, D. Lu, and F. Wang, *Phys. Rev.* **C101**, 034915 (2020), 2004.11745.
- [30] S. Bazak and S. Mrowczynski (2020), 2001.11351.
- [31] V. Vagelli (AMS), *Nuovo Cim.* **C42**, 173 (2019).
- [32] A. Kounine and S. Ting (AMS), *PoS ICHEP2018*, 732 (2019).
- [33] K. Blum, K. C. Y. Ng, R. Sato, and M. Takimoto, *Phys. Rev.* **D96**, 103021 (2017), 1704.05431.
- [34] V. Poulin, P. Salati, I. Cholis, M. Kamionkowski, and J. Silk, *Phys. Rev.* **D99**, 023016 (2019), 1808.08961.
- [35] J. Cleymans and H. Satz, *Z. Phys. C* **57**, 135 (1993), hep-ph/9207204.
- [36] P. Braun-Munzinger, V. Koch, T. Schäfer, and J. Stachel, *Phys. Rept.* **621**, 76 (2016), 1510.00442.
- [37] H. Gutbrod, A. Sandoval, P. Johansen, A. M. Poskanzer, J. Gosset, W. Meyer, G. Westfall, and R. Stock, *Phys. Rev. Lett.* **37**, 667 (1976).
- [38] L. Csernai and J. I. Kapusta, *Phys. Rept.* **131**, 223 (1986).
- [39] P. Danielewicz and G. Bertsch, *Nucl. Phys. A* **533**, 712 (1991).
- [40] H. Sato and K. Yazaki, *Phys. Lett. B* **98**, 153 (1981).
- [41] R. Scheibl and U. W. Heinz, *Phys. Rev. C* **59**, 1585 (1999), nucl-th/9809092.
- [42] S. Mrowczynski, *Acta Phys. Polon. B* **48**, 707 (2017), 1607.02267.
- [43] K.-J. Sun and L.-W. Chen, *Phys. Rev. C* **95**, 044905 (2017), 1701.01935.
- [44] L. Zhu, C. M. Ko, and X. Yin, *Phys. Rev. C* **92**, 064911 (2015), 1510.03568.
- [45] H. Liu, D. Zhang, S. He, N. Yu, and X. Luo (2019), 1909.09304.
- [46] Y. B. Ivanov and A. Soldatov, *Eur. Phys. J. A* **53**, 218 (2017), 1703.05040.
- [47] S. Sombun, K. Tomuang, A. Limphirat, P. Hillmann, C. Herold, J. Steinheimer, Y. Yan, and M. Bleicher, *Phys. Rev. C* **99**, 014901 (2019), 1805.11509.
- [48] Y. Oh, Z.-W. Lin, and C. M. Ko, *Phys. Rev. C* **80**, 064902 (2009), 0910.1977.
- [49] S. Cho, T. Song, and S. H. Lee, *Phys. Rev.* **C97**, 024911 (2018), 1511.08019.
- [50] D. Oliinychenko, L.-G. Pang, H. Elfner, and V. Koch, *Phys. Rev. C* **99**, 044907 (2019), 1809.03071.
- [51] J. Adam et al. (STAR), *Phys. Rev.* **C99**, 064905 (2019), 1903.11778.
- [52] D. Zhang (STAR) (2019), 1909.07028.
- [53] D. Zhang (STAR), in *28th International Conference on Ultrarelativistic Nucleus-Nucleus Collisions* (2020), 2002.10677.
- [54] Z.-W. Lin, C. M. Ko, B.-A. Li, B. Zhang, and S. Pal, *Phys. Rev.* **C72**, 064901 (2005), nucl-th/0411110.
- [55] Y. He and Z.-W. Lin, *Phys. Rev.* **C96**, 014910 (2017), 1703.02673.
- [56] M. Gyulassy and X.-N. Wang, *Comput. Phys. Commun.* **83**, 307 (1994), nucl-th/9502021.
- [57] X.-N. Wang and M. Gyulassy, *Phys. Rev.* **D44**, 3501 (1991).
- [58] B. Zhang, *Comput. Phys. Commun.* **109**, 193 (1998), nucl-th/9709009.
- [59] B.-A. Li and C. M. Ko, *Phys. Rev.* **C52**, 2037 (1995), nucl-th/9505016.
- [60] L. Adamczyk et al. (STAR), *Phys. Rev.* **C96**, 044904 (2017), 1701.07065.
- [61] S. S. Adler et al. (PHENIX), *Phys. Rev.* **C69**, 034909 (2004), nucl-ex/0307022.
- [62] B. Abelev et al. (ALICE), *Phys. Rev.* **C88**, 044910 (2013), 1303.0737.
- [63] M. Gyulassy, K. Frankel, and E. a. Remler, *Nucl. Phys.* **A402**, 596 (1983).
- [64] L.-W. Chen, C. Ko, and B.-A. Li, *Nucl. Phys. A* **729**, 809 (2003), nucl-th/0306032.
- [65] K.-J. Sun and L.-W. Chen, *Phys. Lett.* **B751**, 272 (2015), 1509.05302.
- [66] P. E. Hodgson, (Clarendon, Oxford) p. 453 (1971).
- [67] G. Ropke, *Phys. Rev.* **C79**, 014002 (2009), 0810.4645.
- [68] L. Adamczyk et al. (STAR), *Phys. Rev. Lett.* **121**, 032301 (2018), 1707.01988.